

Molecular Modeling of the Solvent Structuring of Chloroform around Cellulose Triacetate

Isseki Yu, Kazuyuki Iwata, Kazuyoshi Ueda,* and Haruo Nakayama

Department of Material Science, Faculty of Engineering, Yokohama National University, 79-5 Tokiwadai, Hodogaya-ku, Yokohama 240-8501

Received May 2, 2003; E-mail: k-ueda@ynu.ac.jp

A molecular dynamics simulation of the hexamer units of cellulose triacetate (CTA) in chloroform was performed to investigate the solvent structuring and dynamics behavior of chloroform molecules around the CTA polymer. During the simulation, a large fluctuation in the main chain conformation of CTA was observed in this solvent. Moreover, ring puckering of the glucose unit was also observed. In order to investigate the solvent structuring of chloroform around the solute molecule, the site-specified radial distribution function and the average velocity of the solvent atoms were precisely analyzed as a function of the distance from the CTA site. The results were compared with that obtained in our previous simulation of CTA in DMSO. The comparison showed that some DMSO molecules were strongly attracted by CTA sites, such as acetyl methyl residue, while the chloroform molecules were weakly attracted by the carbonyl oxygen of CTA. These differences affect the stability of the conformation of CTA in different solvents. In chloroform, the conformation of acetyl residues, especially at the 6 position, were rotating widely in every monomer unit, which caused a large fluctuation on the main-chain conformation. On the other hand, all acetyl side chains maintained a stable conformation in DMSO because of the strong association of DMSO molecules to the acetyl residue of CTA. The role of the solvent effects on the conformation of the polymer in solution was considered at the molecular level in this work.

Solvation is one of the important factors which affects the molecular conformation in solution. Many experimental studies have been made to obtain information about solvation in relation to the molecular conformation in various kinds of solvents. However, the microscopic picture of solvation, such as, how and where the solvent molecules solvate to the polymer molecule, has still not yet been fully investigated. In order to elucidate molecular-level information about solvation, we have been studying a series of works by using molecular dynamics simulations on some polymer solutions.

In the case of carrageenan in water,[1–3] it has been found that water produced a specific hydration structure with a carrageenan molecule, where a water molecule bound to two sugar rings simultaneously via a hydrogen-bond network. This specific hydration was considered to stabilize the solution conformation of carrageenan in water toward a structure that is close to that found in the crystal structure. In our recent work, we performed a molecular dynamics simulation of cellulose triacetate (CTA) in dimethyl sulfoxide (DMSO)[4] and investigated the solvent structuring of DMSO molecules around the solute molecule in detail. It showed that some DMSO molecules strongly coordinate with CTA at some points, especially at acetyl methyl residues of CTA. Moreover, it was found that those DMSO molecules frequently form a bridge-type interaction between acetyl residues at adjoining glucose rings. These DMSO molecules would play an important role to stabilize the relative orientation of these rings and, as a result, further stabilize the whole main-chain conformation to be an elongated structure in a DMSO solution, as was suggested by many experimental studies, such as light scattering and viscosity.

Cellulose triacetate is one of the main cellulose derivatives that is commercially important in film and fiber industries.[5] In these fields, data concerning the solution properties of CTA in different solvents are important because they give basic information for improving the quality of the products. Among these solvents, chloroform is as important as DMSO in basic studies of the CTA properties. The results obtained in chloroform are frequently discussed along with that of DMSO, because they are good examples with opposite properties on polarity in their solvents. However, most research has been focused on the macroscopic properties, such as the viscosity and reology of the solution. Although NMR is one of a few experimental methods which can detect information about microscopic interactions, reports concerning the CTA solution are still few in number.[6–8] Molecular dynamics simulation is one of the powerful methods to investigate microscopic molecular information when it is used in combination with NMR. However, an investigation of the solution properties of CTA in chloroform by using a molecular dynamics simulation has not yet been performed.

In this work, we performed a molecular dynamics simulation of CTA in chloroform for the first time, and the results were discussed along with those of DMSO obtained in our previous work.[4] Especially, we considered not only the difference in the static properties of the spatial coordination between these two solvents, but also the dynamic properties, such as the velocity and residence time when they are trapped within the solvation shell around the acetyl residues. From these data, the differences in the coordination behavior of these two solvents, and the solvent effects on the conformation of CTA can be considered.

Recently, CTA becomes to attract attention in new applica-

Published on the web December 15, 2003; DOI 10.1246/bcsj.76.2285

tion fields like optical uses. In this usage, the microscopic conformations of the main chain and the side chain acetyl residues are directly related to controlling the functions, such as the refractive indices of CTA film. The molecular-level information obtained from molecular dynamics simulations will be expected to become more important in the future for developing new functions of cellulose derivatives. Moreover, it is also expected to provide useful information for the development of well-designed new nano-structure materials by controlling the three-dimensional structure of this polymer.

Nomenclatures and Calculation Procedures

A model of cellulose triacetate with hexamer units was used in this simulation. Their monomer units are numbered sequentially from the non reducing end. Atomic nomenclatures of the CTA monomer unit are shown in Fig. 1. In the text, these atom names are expressed with their residue number, which is attached before each atom name. The dihedral angles of the glycosidic bonds are defined as ϕ: *n*C2–*n*C1–*n*O1–($n+1$)C4 and ψ: *n*C1–*n*O1–($n+1$)C4–($n+1$)C3, n = 1–5, respectively.

Molecular mechanics and molecular dynamics calculations were all performed using the CHARMM25[9] program in a manner similar to that described in a previous paper.[4] Ha's force field parameter set, which was developed for carbohydrate,[10] was used for pyranose rings of CTA with the combination of our parameters obtained for the acetyl residue.[4] The force field parameter for chloroform, that was used, was developed by Dietz et al.[11,12] This model treats chloroform as a rigid molecule with C, H and three Cl, which are named CFM, HFM, ClF1, ClF2, and ClF3 in this study, respectively.

The initial conformation of the hexamer CTA was the same as described in a previous paper.[4] That is, the glycosidic dihedral angles of the CTA hexamer were all set at the value of ($\phi = 180°$, $\psi = 120°$), which locates at the global minimum in the adiabatic potential energy map of the dimer unit of CTA. The acetyl side-chain conformations were all set at *gt* for the 6 position, and *cis* at the 2 and 3 positions. This hexamer was put at the center of a 55 Å × 55 Å × 80 Å box filled with pre-equilibrated chloroform molecules, and then the overlapped solvents with a CTA hexamer were eliminated. The resulting 1785 chloroform molecules were included in the simulation box. Periodic boundary conditions were assigned to the box.

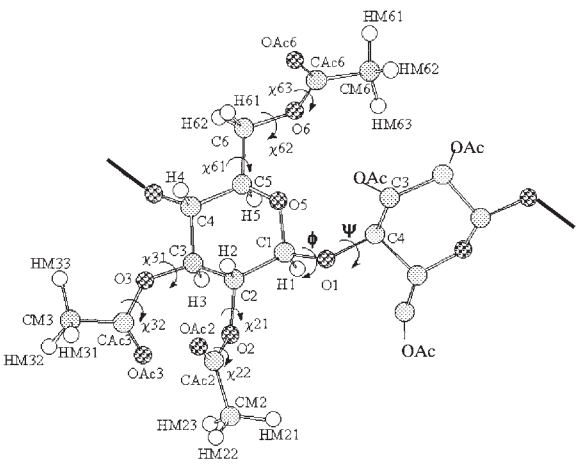

Fig. 1. Nomenclature of the monomer unit of cellulose triacetate.

The solution density of the CTA hexamer in chloroform was set at 1.475 g/cm^3 according to the experimental value of Moore.[13] The trajectories were integrated using the Verlet method with a time step of 1 fs by the NVE ensemble. The electrostatic interaction was calculated using the Ewald method.[14] The system was equilibrated at 300 K for the first 20 ps by restraining all glycosidic angles of ϕ and ψ, and a following the free simulation of 1000 ps was performed for analysis.

Results and Discussion

Conformation of CTA in Chloroform. Before investigating the solvation of chloroform around CTA, we analyzed the

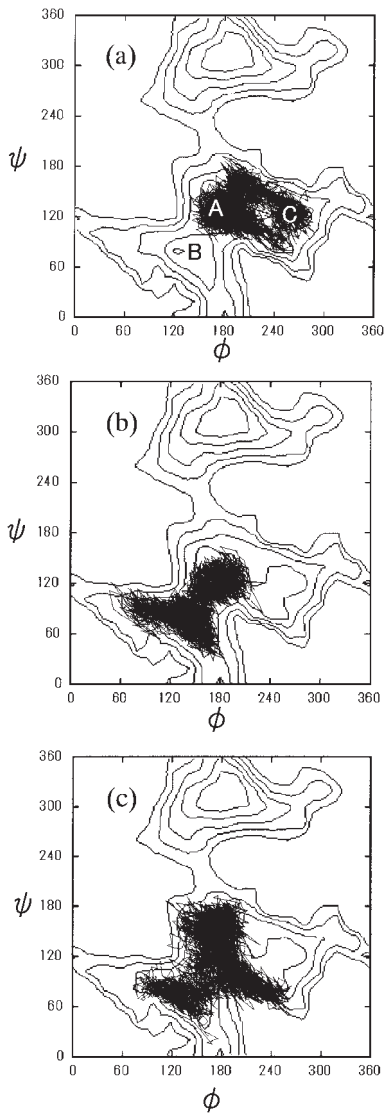

Fig. 2. Trajectories of the ϕ and ψ dihedral angles of glycosidic linkages for the hexamer CTA in chloroform. The trajectories were superimposed on the adiabatic potential energy map obtained in the previous work. They were all started from the global minimum point at $\phi = 180°$, $\psi = 120°$. The glycosidic linkages are between (a) CTA2 and CTA3, (b) CTA3 and CTA4, and (c) CTA4 and CTA5. The local minima of the adiabatic potential energy map were indicated by capitol letters from A to C.

dynamics of the main chain conformation of CTA in chloroform. Figure 2 shows the trajectories of the glycosidic dihedral angles of ϕ and ψ which were superimposed upon the adiabatic potential energy map previously calculated for the dimer CTA.[4] To avoid the end effect of the chain, the results of the terminal residues were not included in this analysis. It can be seen that the values of ϕ and ψ did not stay within the original low energy region A, but were moving around widely among the low energy wells of A, B, and C. This indicates that there is a large fluctuation on the main-chain conformation in chloroform. On the other hand, our previous work in DMSO showed that the trajectories of CTA stayed in the small area within the original position A at all times investigated. The difference in the main-chain conformation suggests the different behavior of the role for these two solvents on the stabilization of the CTA conformation. Kamide and Saito[15] measured the unperturbed chain dimension of CTA in popular solvents of DMSO, DMAc, acetone, THF and so on. Their results showed that the unperturbed chain dimension of the CTA molecule become larger in more polar solvents. This means that CTA behaves as a more flexible chain in a less polar solvent. This agrees with our result that the conformation of CTA in chloroform, which is a less polar solvent than DMSO, shows a large fluctuation in the main-chain conformation.

A further analysis on the conformation of CTA in chloroform revealed that the conformational change occurred not only in the main chain conformation, but also in the pyranose ring conformation. In order to investigate the conformational change of the pyranose ring, we calculated the puckering parameter determined by Cramer and Pople.[16] Figure 3 shows the time courses of the puckering parameter θ calculated for the pyranose rings at the central part of the hexamer CTA. In Fig. 3(a), it can be seen that the ring conformation shifts from the $^4C_1$ conformation (θ is around 0°) to a boat conformation (θ is around 90°) at 700 ps, and then back to the original chair conformation again at 800 ps. Similarly, the ring conformation at the 4th residue of CTA (CTA 4) shifts from the $^4C_1$ conformation to a boat conformation at 550 ps, and never back to the chair conformation within the time range of our 1000 ps simulation. The ratio of the population between these two ring conformations could not be estimated in this analysis because of the insufficient number of inter-conversion of the puckering parameter observed in our 1000 ps simulation time.

Ogura et al. measured the infra-red dichroism of CTA film,

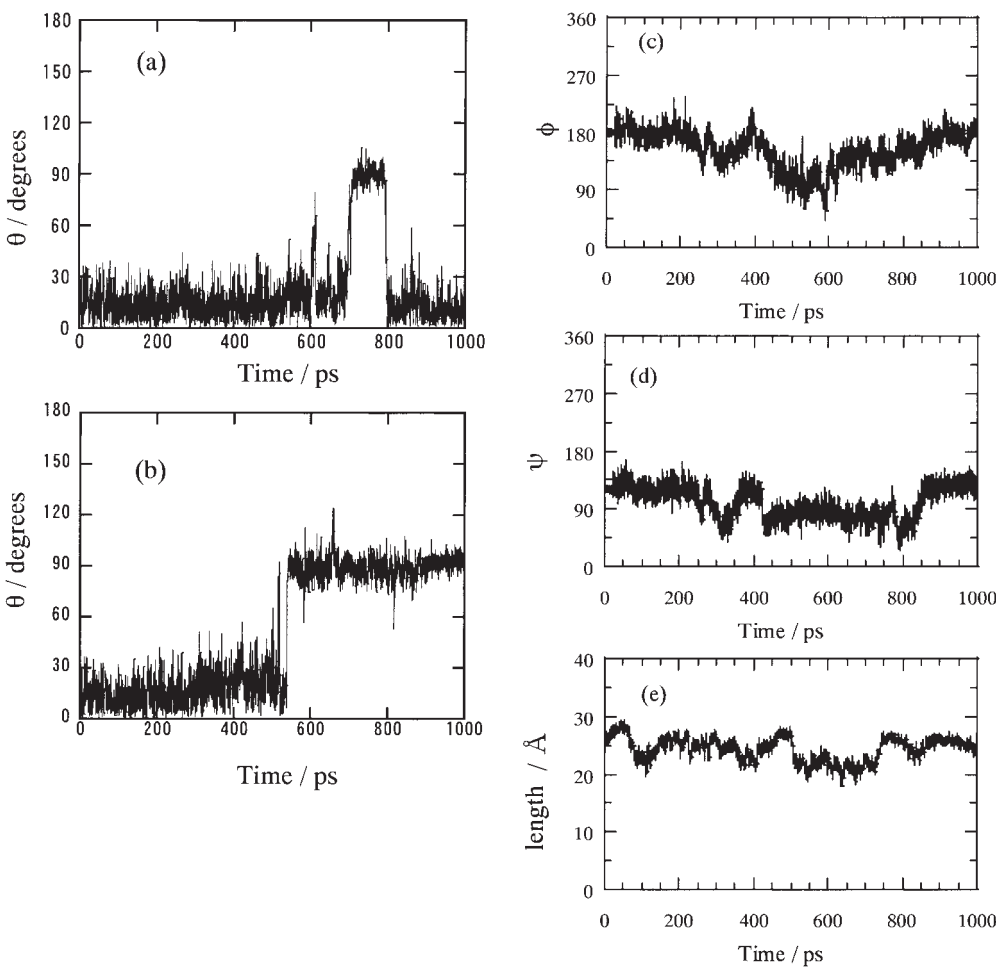

Fig. 3. Time histories of the puckering parameter θ calculated for the residues of (a) CTA3 and (b) CTA4 in chloroform. The value of $\theta = 0°$ indicates that the ring conformation corresponds to $^4C_1$, and $\theta = 90°$ corresponds to boat conformations, respectively. Time histories of the glycosidic dihedral angles ϕ (c) and ψ (d), and the end-to-end length between C4 of CTA1 and C1 of CTA6 (e).

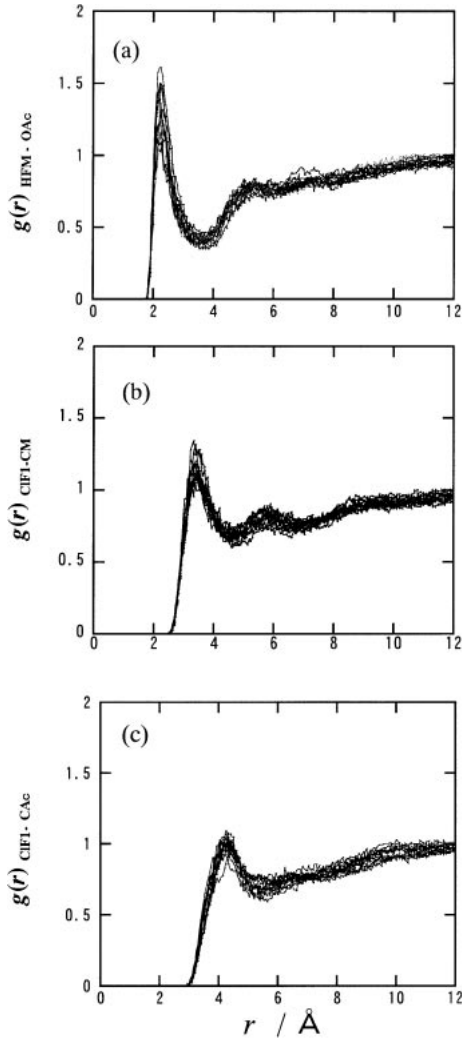

Fig. 4. Radial distribution function, $g(r)$, of chloroform around the acetyl residues of hexamer CTA. The radial distribution functions were calculated for (a) hydrogen atoms of chloroform (HFM) around the acetyl carbonyl oxygens of CTA (OAc), and for (b) chloride atom of chloroform (ClF1) around acetyl methyl carbons of CTA (CM), and for (c) chloride atom of chloroform (ClF1) around acetyl carbonyl carbons of CTA (CAc), respectively. The lines indicated the results calculated for all acetyl residues from CTA2 to CTA5, and they are simply superimposed on the same figure without any distinction of the acetyl position and the residues.

and observed a large change in the dichroic ratio of the C1–H group at around 30 °C.[17] They estimated that this change could be attributed to the transition of a pyranose ring from a chair to a boat conformation. Moreover, they investigated the NMR spectra of CTA in chloroform at temperatures ranging from −11 °C to 130 °C, and observed that two peaks of the acetyl protons at the 2- and 3-positions merged to a single peak according to the increment of the temperature.[18] They explained that this is because of the occurrence of the transition from the $^4C_1$ chair to a boat conformation because this transition makes the steric hindrance of the acetyl methyl rotation at 2- and 3-positions equivalent. Our results provide support to their observation.

Ring puckering may affect the main chain conformation of CTA. The time histories of the glycosidic dihedral angles of ϕ and ψ between the 3rd and 4th residues were investigated and are shown in Figs. 3(c) and (d). The dihedral angles were fluctuating with the time, but the cooperative movement between these angles and the ring puckering was not observed. The time history of the end-to-end length of the hexamer CTA is also shown in Fig. 3(e). A large fluctuation of this length indicates the conformational flexibility of the main chain in this solvent. However, no cooperative movement between the change in the main chain conformation and the ring puckering was observed.

On the other hand, in DMSO, we did not observe any transition of the glucose ring during a calculation time of 1000 ps. These results again suggest that solvation has a great effect on the stability not only of the polymer conformation, but also the ring conformation in the solvent. In the next section, we consider the solvation structure in more detail.

Analysis of the Solvation. The solvation was found to have a great effect on the conformation of CTA in solvents. In order to investigate how in the solvation the chloroform molecules are spatially oriented around CTA, the radial distribution functions (RDF) of chloroform molecules were analyzed around some selected atom sites of CTA. After considering the combination of various types of atom pairs, one was selected from the atom in CTA as a site of RDF analysis, and the other was an atom selected from chloroform, the largest first solvation peak of RDF was observed between the hydrogen atoms of chloroform (HFM) and the acetyl carbonyl oxygen atoms of CTA (OAc). The results were shown in Fig. 4(a). The ring puckering observed in Fig. 3 may affect to the solvent structuring around CTA. Therefore, the effect was investigated by analyzing the RDF at two different time regions of the $^4C_1$ and $^2S_0$ conformations. However, the obtained RDF curves were almost similar in two different regions. This indicates that the change in the ring conformation does not give such a large distortion to the solvation structure of chloroform around CTA. This may partly be because of the small value of RDF obtained for chloroform around CTA, and partly because of the location of acetyl residues, which were rather apart from the ring position. Therefore, the all of the time regions were used in the following analysis. Because no large difference was observed in the RDF curves among the different positions of the acetyl residues, the results obtained from all OAc sites on the residues from CTA2 to CTA5 were simply superimposed in the figure. The end residues were not again included so as to avoid the end effects. Their first peaks located at 2.3 Å and their intensities were scattered from 1.09 to 1.61. The average of these values is given in Table 1 along with the coordination number of the solvents within the first peak. The value of the intensity indicates that the solvation of chloroform to CTA is not strong.

Similarly, the second largest peak of RDF was observed between chloride atoms of chloroform (ClF1) and acetyl methyl carbon atoms of CTA (CM). The results are shown in Fig. 4(b). Because all three chloride atoms in the same chloroform molecule are equivalent spatially, no difference was observed in RDF for these chloride atoms. The intensities of their

Table 1. Characteristic Features of the First Solvation Shell Obtained by Radial Distribution Function between the Selected CTA Atom Sites and the Solvent Atoms of DMSO and Chloroform

Atom pairs Atoms of CTA site–Atoms of solvent	Average distance of first peak r/Å	Average value of first peak $g(r)$	Average number of atoms within the first peak n
Chloroform			
Acetyl carbonyl O (OAc)–HFM	2.3	1.3	0.83
Acetyl methyl C (CM)–ClF1	3.4	1.2	2.3
Acetyl carbonyl C (CAc)–ClF1	4.3	1.0	3.1
DMSO			
Acetyl methyl C (CM)–ODM	3.0	2.8	2.1
Acetyl carbonyl C (CAc)–ODM	3.5	1.1	1.9
Acetyl carbonyl O (OAc)–CD1	3.1	1.6	1.9

first peak at a radius of 3.4 Å were scattered from 1.05 to 1.35. The dependence of these interactions on the position of the acetyl residues was again not seen in these cases. The third largest peak of RDF was found between ClF1 and CAc. In this case, the intensities of the first peak are close to unity, which indicates that the interaction between these two atoms is weak. Kamide et al. measured the chemical shift of the acetyl methyl proton and carbonyl carbon atoms of CTA in various solvents using pulse-Fourier ^{1}H and ^{13}C NMR.[19] From these chemical shifts, they estimated that the chloride atom of chloroform would coordinate to the acetyl carbonyl carbon of CTA. Although they only observed the interaction between the acetyl carbonyl carbon of CTA and chloroform, our simulation suggests that other types of coordination exist between HFM and OAc, and ClF1 and CM.

However, it should be emphasized that all of these interactions found in chloroform are intrinsically weak, even though they showed interactions, as discussed above. In our previous work of CTA in DMSO, the strongest RDF peek was observed at a distance of around 3.0 Å with an average intensity of 2.8 between the acetyl methyl carbon atoms and the DMSO oxygen. This was interpreted as meaning that the C–H···O type hydrogen bond interaction[20–23] exists between the acetyl methyl residue and the DMSO oxygen atom. In chloroform, on the other hand, even the largest first RDF peaks have an average value of only 1.3 between OAc and HFM. This indicates that the interaction between the solvents and the solute is weak compared to that of DMSO.

The Movement of the Solvents around CTA. The radial distribution function is a convenient tool to know how the solvent molecule orients around the CTA molecule spatially on the average. However, it does not give any dynamical information about how the solvated molecules move in and out of the solvation shell. This information provides a clear picture of the coordination behavior of the solvent to the CTA sites. In this section, we consider the dynamics behavior of the solvent molecules around CTA in more detail.

In order to understand the dynamics of the solvent, the speed of the solvent, $|\mathbf{v}(r)|$, was investigated as a function of the distance r from a selected atom site of CTA in DMSO and in chloroform. The values of the speed obtained in DMSO and in chloroform were averaged over the whole simulation time. The averaged values, $\langle|\mathbf{v}(r)|\rangle$, are shown in Figs. 5(a) and (b), respectively. In these figures, only typical cases for the pairs that showed the strongest interaction in both solvent systems were calculated. That is, the result obtained in DMSO for the pairs between the acetyl methyl carbon at the 6-position of the 4th pyranose residue (4CM6) and oxygen of DMSO (ODM) is shown in Fig. 5(a), and the result obtained in chloroform for the pairs between the acetyl carbonyl oxygen at the same position (4OAc6) and the hydrogen of chloroform (HFM) is shown in Fig. 5(b).

At a short distance of r, $\langle|\mathbf{v}(r)|\rangle$ has no value because of exclusion of the solvent molecules by the van der Waals repulsion from the CTA molecules. Apart from the exclusive regions, $\langle|\mathbf{v}(r)|\rangle$ becomes constant with a value of 4.6×10^2 m/s for ODM and 4.0×10^2 m/s for HFM. This indicates that the averaged speeds of the solvent molecules are almost constant in all regions in both solvents, although the value of $\langle|\mathbf{v}(r)|\rangle$ in DMSO is slightly larger than that in chloroform. In other words, there are no differences in the averaged speed of the molecules between in the first solvation shell and in the other parts of the region.

Because the value of $\langle|\mathbf{v}(r)|\rangle$ is the average speed of the solvent, it can not give information about the direction of the movement of the solvent molecules. However, it is interesting to know the behavior of the solvent molecules if they are approaching to CTA or not. In order to obtain this information, we calculated $\langle\mathbf{v}_r(r)\rangle$, the velocity of the solvents along the radial direction from the selected site atom of CTA. The results are also shown in Figs. 5(a) and (b). The sign was defined such that it takes a positive value when the solvent atom goes away from CTA.

Interestingly, we can see a strong relationship between $\langle\mathbf{v}_r(r)\rangle$ and the RDF curves in both solvents. In the first solvation shell of RDF, the value of $\langle\mathbf{v}_r(r)\rangle$ showed a sharp positive peak at the first half region, and showed negative minima at the latter half region. Furthermore, $\langle\mathbf{v}_r(r)\rangle$ had a slightly positive value at the first minimum of RDF, and then converged to 0 with an increment of the distance from the site of CTA.

The first positive value of $\langle\mathbf{v}_r(r)\rangle$ indicates the tendency of the solvents to go away from the CTA site because of the van

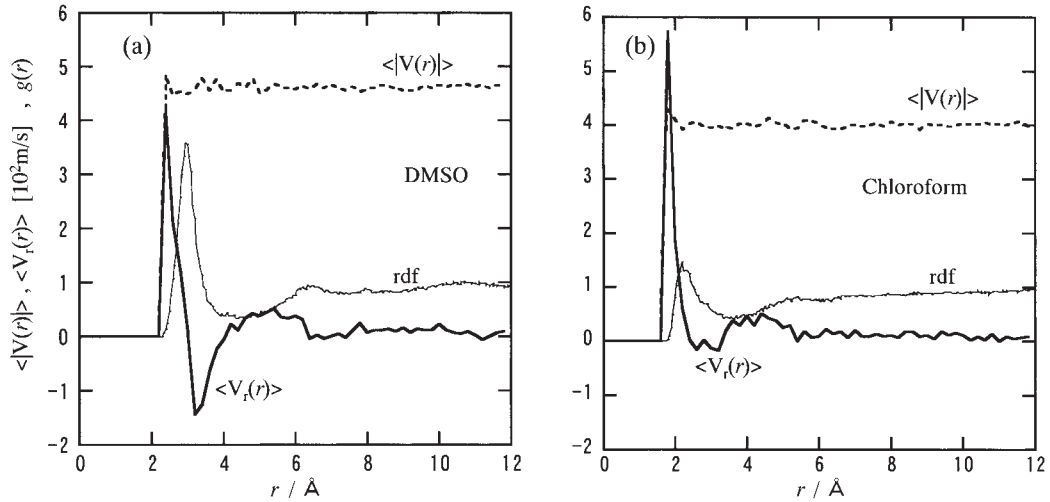

Fig. 5. Radial distribution function, $g(r)$, and the average speed of the solvent atoms, $\langle|\mathbf{v}(r)|\rangle$, were shown as a function of the distance from a selected CTA atom site. Average velocity of the solvent atoms in the spherical shell along the radial direction, $\langle\mathbf{v}_r(r)\rangle$, were also calculated as a function of the distance from a selected CTA atom site. (a) Oxygen of DMSO (ODM) was selected as a solvent atom and acetyl methyl carbon at 6 position in CTA4 (4CM6) was selected as an atom site of CTA. (b) Hydrogen of chloroform (HFM) was selected as a solvent atom and acetyl carbonyl oxygen at 6 position in CTA4 (4OAc6) was selected as an atom site of CTA.

der Waals repulsion by the CTA. On the other hand, the negative value of $\langle\mathbf{v}_r(r)\rangle$ indicates that the solvents tend to approach toward the CTA site. These results indicate that the molecules in the first solvation shell would be forced to be detained within the shell. By comparing the depth of the minima of $\langle\mathbf{v}_r(r)\rangle$ for both solvents, DMSO has a deeper minimum compared to that of chloroform. This indicates that DMSO molecules in this region are more attracted toward the CTA site. On the other hand, chloroform is slightly attracted toward the CTA site. By summarizing the above results, it can be concluded that the DMSO molecules within the first solvation shell are strongly detained in this region, while chloroform is weakly detained. The characteristic values of $\langle|\mathbf{v}(r)|\rangle$ and $\langle\mathbf{v}_r(r)\rangle$ are summarized along with their positions in Table 2.

It is also interesting to know how frequently the solvent molecules move in and out from the first solvation shell. For this purpose, we calculated the time history of the solvent atoms detained inside the first solvation shell. The results are shown in Fig. 6. As an example, the calculations were performed within an arbitrarily selected time range of 200 ps from 600 ps to 800 ps dynamics run. In the figure, solvent atoms are expressed by their sequential numbers. Because all of the solvent atoms have their sequential number in our simulation, the horizontal lines appear at their numbered position during the time that the atom exists inside of the solvation shell. Figure 6(a) shows the DMSO oxygens (ODM) existing within the first solvation shell around the acetyl methyl carbon 4CM6 of CTA. Long horizontal lines can be seen in the figure. This indicates that the solvent molecules, once detained in the first solvation shell, tend to stay as they are for a long time. In contrast, chloroform hydrogens (HFM) around the 4OAc6 of CTA have a short detaining time and a high frequency of exchange, as shown in Fig. 6(b).

Because molecules repeat to move in and out from the solvation shell, the average detained time per one access was calculated by dividing the total detained time by the number of egressions and ingressions found in Fig. 6. The total detained time of all DMSO oxygens (ODM) around 4CM6 in the period

Table 2. Comparison of the Average Speed of Solvent, $\langle|\mathbf{v}(r)|\rangle$, and the Velocity of the Solvent along the Radial Direction from the Selected Site Atom of CTA, $\langle\mathbf{v}_r(r)\rangle$, in DMSO and Chloroform

	Solvents and selected sites	
	DMSO **ODM–4CM6** (DMSO oxygen–acetyl methyl carbon at 6-position of 4th residue of CTA)	**Chloroform** **HFM–4OAc6** (Chloroform hydrogen–acetyl carbonyl oxygen at 6-position of 4th residue of CTA)
$\langle\|\mathbf{v}(r)\|\rangle/10^2$ ms^{-1}	4.6	4.0
$\langle\mathbf{v}_r(r)\rangle/10^2$ ms^{-1}	4.2	5.7
(Radius at first peak)	($r = 2.4$ Å)	($r = 1.8$ Å)
$\langle\mathbf{v}_r(r)\rangle/10^2$ ms^{-1}	−1.4	−0.2
(Radius at first minimun)	($r = 3.2$ Å)	($r = 3.2$ Å)
$\langle\mathbf{v}_r(r)\rangle/10^2$ ms^{-1}	0.5	0.5
(Radius at second peak)	($r = 5.4$ Å)	($r = 4.4$ Å)

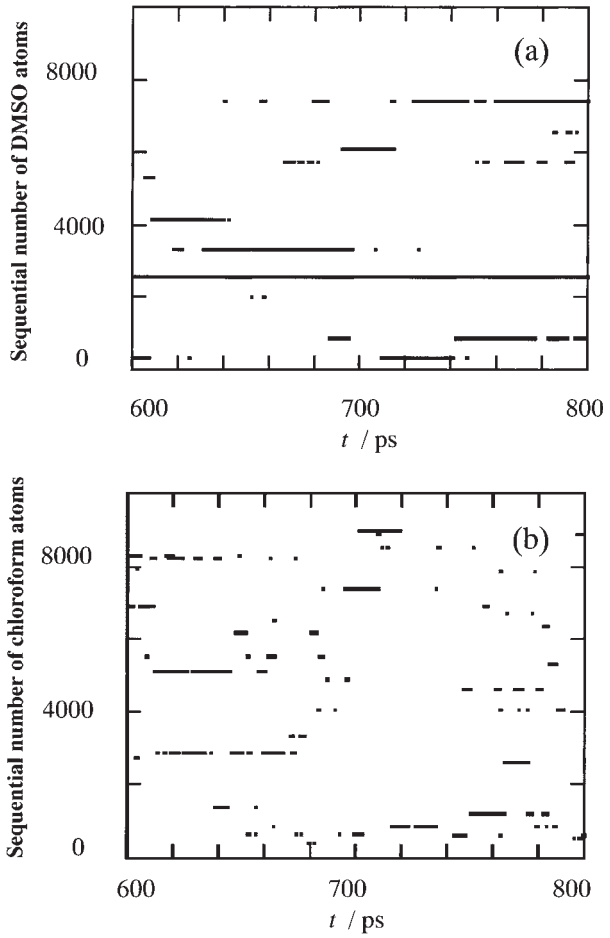

Fig. 6. Time histories of the solvent atoms existing within the first solvation shell. The horizontal lines appear at their numbered position during the time that the solvent atom exists inside the solvation shell. (a) DMSO oxygen (ODM) inside the first solvation shell around 4CM6, and (b) chloroform hydrogen (HFM) inside the first solvation shell around 4OAc6, are shown. The ordinate is the sequential serial number of solvent atoms defined in this work.

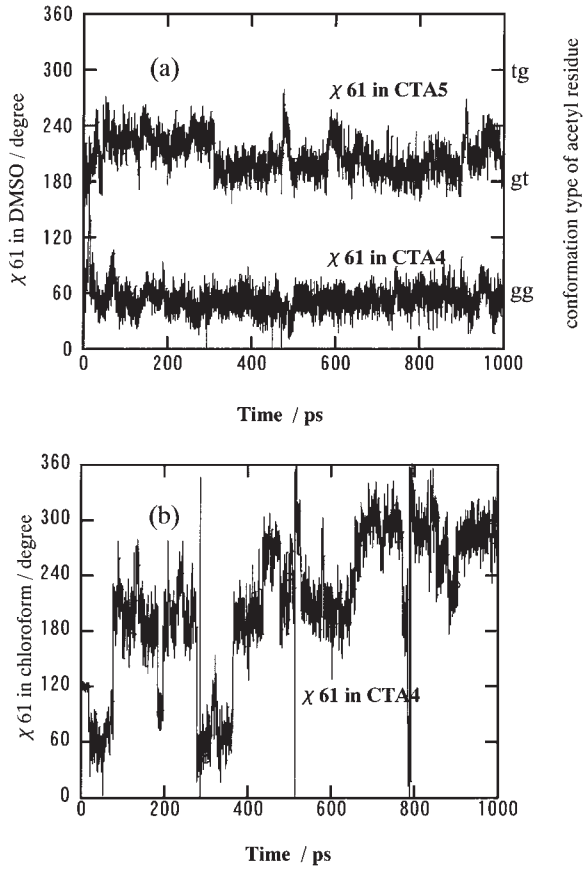

Fig. 7. Time histories of the dihedral angles of (a) χ61 in CTA4 and CTA5 in DMSO, and (b) χ61 in CTA4 in chloroform.

of 200 ps in Fig. 6(a) was 458 ps in DMSO, while that of chloroform hydrogen (HFM) around 4OAc6 in Fig. 6(b) was 183 ps in chloroform. Because the number of egressions and ingressions for ODM around 4CM6 was 180 times in DMSO and that of HFM around 4OAc6 in chloroform was 213 times in the same figures, the average detained time per one access became 2.54 ps for ODM and 0.86 ps for HFM, respectively. This quantitatively indicates that the DMSO stays three-times longer in the first solvation shell than chloroform. Moreover, in DMSO, a molecule once detained in the solvation shell can be seen to repeat the egressions and ingressions to the same acetyl residue as was seen in a figure like a straight line (Typical example, see the DMSO molecule of sequence number 2300 in Fig. 6(a)). Actually, in Fig. 6(a), only 11 DMSO oxygen is repeatedly detained in the first solvation shell, while there are 35 hydrogen atoms of chloroform in Fig. 6(b). Therefore, the solvation shell around the acetyl methyl carbon 4CM6 of CTA is almost occupied every time by the same DMSO atom. In contrast, chloroform molecules are exchanged one after another at short intervals.

Local Motion of Acetyl Residues. In previous sections, we clarified the difference in the solvation behavior for two solvents of DMSO and chloroform around the acetyl residue of CTA molecules. These different solvation behaviors should affect to the local motion of the acetyl side-chain conformation. Figure 7 compares the time histories of the dihedral angles of the acetyl residue at the 6 positions (χ61) in both solvents. The time histories of χ61 at the residues of CTA4 and CTA5 in DMSO are shown in Fig. 7(a). It can be seen that the dihedral angles both maintained their values well at around 60° (*gg*) and 180° (*gt*), respectively. As mentioned in our pervious work, these two conformations were the lowest energy conformations of the acetyl residue for the CTA monomer. The rotation of the acetyl residue conformation in DMSO would be suppressed by the solvation of DMSO molecules, and stabilized at one of the lowest energy conformations. In contrast, χ61 in chloroform would not stay at its initial conformation, but would rotate the dihedral angles from one after another, as shown in Fig. 7(b). This indicated that, in chloroform, the acetyl residue at the 6 position was frequently rotating among its dihedral conformations. Other dihedral angles of the acetyl residue at the 6 position, χ62 (*n*C5–*n*C6–*n*O6–*n*CAc6) and χ63 (*n*C6–*n*O6–*n*CAc6–*n*OAc6), were also investigated. The dihedral angle χ62 did not keep a constant value in both solvents, but the fluctuation of χ62 in chloroform was much larger than that in DMSO. On the other hand, χ63 kept a value of around 0° in

both solvents.

Other acetyl residues at the 2 and 3 positions, the dihedral angles of χ21 (*n*H2–*n*C2–*n*O2–*n*CAc2) and χ31 (*n*H3–*n*C3–*n*O3–*n*CAc3), were also investigated. They were swinging around the *cis* position in both solvents, but sometimes had short excursions toward the *trans* position at some acetyl residues in chloroform. The above results indicated the difference between these two solvents on the role to stabilize the conformation of acetyl chain, especially at the 6 position. In DMSO, most of the acetyl residue conformations maintained a fixed conformation at all of the times investigated. However, in chloroform, the acetyl side chain moved rather freely, rotating especially at the 6 position, which is a similar behavior to that which we observed in the vacuum simulation.

Kamide et al. measured the spin-lattice relaxation time (T_1) of the carbonyl carbon atoms of CTA in various solvents using pulse-Fourier ^{13}C NMR.[19] The result showed that in DMSO, T_1 at the 2, 3, and 6 positions showed almost the same values at around 2.3 s. On the other hand, in chloroform, T_1 at the 6 position is 2.83 s, while those of 2, 3 positions are 2.49 and 2.28, respectively. The large T_1 value indicates that the local motion of acetyl residue at the 6 position of chloroform has a larger fluctuation compared to those of the 2 and 3 positions and those of DMSO. Our results are in good agreement with their results, and explain their observation from a molecular level point of view.

Conclusion

By using a molecular dynamics simulation, we investigated the spatial orientation of a solvent atoms around a CTA molecule. Especially, the local motion and the exchange rate of the solvents in the first solvation shell were investigated. From these analyses, it was found that the DMSO molecule forms strong solvation to the acetyl methyl residues, and they are strongly detained within the first solvation shell. A molecule once detained in the solvation shell remains at a place close to the acetyl residue by repeating egressions and ingressions in DMSO. In contrast, chloroform is more frequently exchanging the solvated molecules with one after another around the solvation site at the acetyl residue.

The difference in the extent of solvation around the acetyl residue directly affected the rotational motion of the acetyl side chain. In chloroform, the acetyl side chain at the 6 position was rotating very frequently. This is because the chloroform can not form strong solvation, and thus, can not fix the rotational motion of the acetyl side chain compared to that of DMSO. The large rotational motion of the side chain, especially at the 6 position, would cause a large fluctuation of the main-chain conformation, and occasionally may cause a transformation of the glucose ring conformation.

In this work, we examined the relation between the solvent properties and the polymer conformation from a molecular level point of view by using a molecular dynamics simulation. Solvation around the side chain residue affects to the difference of the CTA conformation in solvents.

The authors thank Daicel Chemical Co. Ltd. for financial support.

References

1 K. Ueda and J. W. Brady, *Biopolymers*, **38**, 461 (1996).
2 K. Ueda, M. Saiki, and J. W. Brady, *J. Phys. Chem. B*, **105**, 8629 (2001).
3 K. Ueda, K. Iwama, and H. Nakayama, *Bull. Chem. Soc. Jpn.*, **74**, 2269 (2001).
4 I. Yu, K. Ueda, and H. Nakayama, *Bull. Chem. Soc. Jpn.*, **76**, 529 (2003).
5 V. Stannett, "Cellulose Acetate Plastics," Temple press, London (1950).
6 Y. Tezuka, *Biopolymers*, **34**, 1477 (1994).
7 Y. Tsunashima and K. Hattori, *J. Colloid Interface Sci.*, **228**, 279 (2000).
8 C. M. Buchanan, J. A. Hyatt, and D. W. Lowman, *J. Am. Chem. Soc.*, **111**, 7312 (1989).
9 B. R. Brooks, R. E. Bruccoleri, B. D. Olafson, D. J. States, S. Swaminathan, and M. Karplus, *J. Comput. Chem.*, **4**, 187 (1983).
10 S. N. Ha, A. Giammona, M. Field, and J. W. Brady, *Carbohydr. Res.*, **180**, 207 (1988).
11 W. Dietz and K. Heinzinger, *Ber. Bunsen-Ges. Phys. Chem.*, **88**, 543 (1984).
12 W. Dietz and K. Heinzinger, *Ber. Bunsen-Ges. Phys. Chem.*, **89**, 968 (1985).
13 W. R. Moore, *J. Polym. Sci., Part C: Polym. Symp.*, **16**, 571 (1967).
14 P. Ewald, *Ann. Phys.*, **64**, 253 (1921).
15 K. Kamide and M. Saito, *Eur. Polym. J.*, **20**, 903 (1984).
16 D. Cremer and J. A. Pople, *J. Am. Chem. Soc.*, **97**, 1354 (1975).
17 K. Ogura, Y. Miyauchi, H. Soube, and S. Nakamura, *Makromol. Chem.*, **176**, 1173 (1975).
18 K. Ogura, H. Soube, M. Kasuga, and S. Nakamura, *J. Polym. Sci., Polym. Lett. Ed.*, **11**, 421 (1973).
19 K. Kamide, M. Saito, K. Kowsaka, and K. Okajima, *Polym. J.*, **19**, 1377 (1987).
20 I. I. Vaisman and M. L. Berkowitz, *J. Am. Chem. Soc.*, **114**, 7889 (1992).
21 T. Steiner and W. Saenger, *J. Am. Chem. Soc.*, **114**, 10146 (1992).
22 S. T. Rao and M. Sundaralingam, *J. Am. Chem. Soc.*, **92**, 4963 (1970).
23 P. Auffinger, S. Louise-May, and E. Westhof, *J. Am. Chem. Soc.*, **118**, 1181 (1996).